Journal of Pharmacy and Pharmacology, 2021, **74**, 1467–1476
https://doi.org/10.1093/jpp/rgab173
Advance access publication 20 December 2021
Research Paper

JPP Journal of Pharmacy and Pharmacology

OXFORD

Development of 3D printed drug-eluting contact lenses

Youssra Moustafa Gadelkareem Mohamdeen[1,2], Atabak Ghanizadeh Tabriz[1,3], Mohammad Tighsazzadeh[1], Uttom Nandi[1,3], Roxanne Khalaj[1,3], Ioannis Andreadis[4], Joshua S. Boateng[1] and Dennis Douroumis[1,3,*]

[1]Faculty of Engineering and Science, School of Science, University of Greenwich, Chatham, Kent, UK
[2]Faculty of Biotechnology, October University for Modern Sciences and Arts (MSA), Cairo, Egypt
[3]CIPER: Centre for Innovation and Process Engineering Research, Kent, UK
[4]Laboratory of Pharmaceutical Technology, Department of Pharmaceutical Sciences, Aristotle University of Thessaloniki, Thessaloniki, Greece

*Correspondence: Dennis Douroumis, Faculty of Engineering and Science, School of Science, University of Greenwich, Chatham Maritime, Chatham Maritime, Chatham, Kent ME4 4TB, UK. Email: d.douroumis@gre.ac.uk

Abstract

Objectives The aim of the work was to introduce 3D printing technology for the design and fabrication of drug-eluting contact lenses (DECL) for the treatment of glaucoma. The development of 3D printed lenses can effectively overcome drawbacks of existing approaches by using biocompatible medical grade polymers that provide sustained drug release of timolol maleate for extended periods.

Methods Hot melt extrusion was coupled with fusion deposition modelling (FDM) to produce printable filaments of ethylene-vinyl acetate copolymer–polylactic acid blends at various ratios loaded with timolol maleate. Physicochemical and mechanical characterisation of the printed filaments was used to optimise the printing of the contact lenses

Key findings 3D printed lenses with an aperture (opening) and specified dimensions could be printed using FDM technology. The lenses presented a smooth surface with good printing resolution while providing sustained release of timolol maleate over 3 days. The findings of this study can be used for the development of personalised DECL in the future.

Graphical abstract

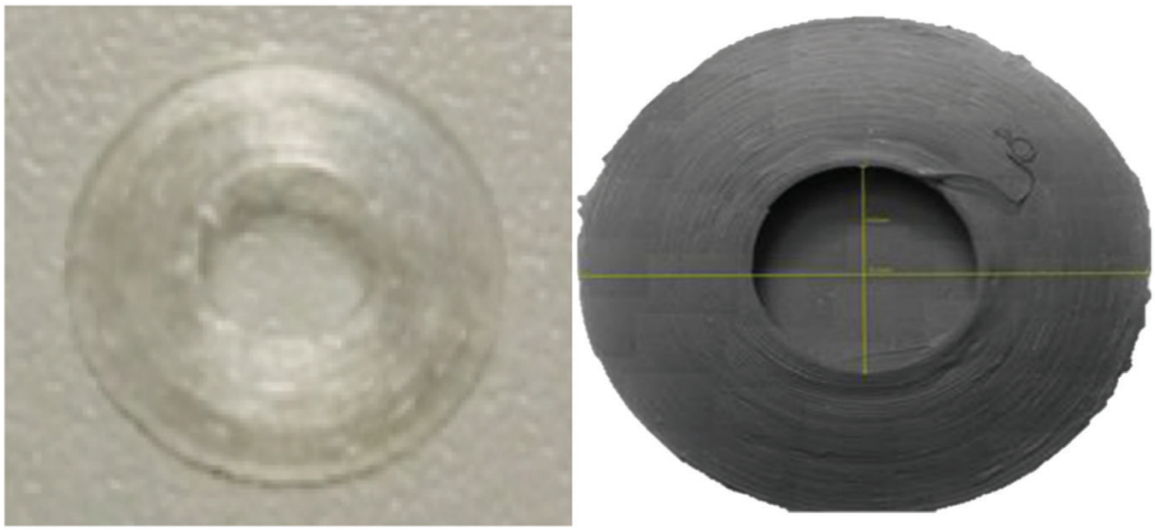

Keywords: 3D printing; fusion deposition modelling; hot melt extrusion; contact lenses; medical biodegradable; glaucoma

Introduction

Glaucoma is considered to be the leading cause of irreversible vision loss. There are nearly 80 million people that are diagnosed with glaucoma worldwide.[1, 2] The disease affects mainly the optic nerve of the eye where its gradual damage could eventually cause complete loss of vision.

Topical medications, which involve a single drug substance or a combination thereof, are used as first line of defence for glaucoma treatment and management. However, the administration of topical dosage forms such as eye drops are not very effective as physiologic and anatomic factors including tear turnover, blinking, induced lacrimation, tear film and solution

Received: 6 September 2021. **Revised:** November 5, 2021. **Accepted:** 25 November 2021.

drainage are the limiting factors affecting the bioavailability. The tear film is considered the first limiting barrier because it has a high turnover rate and rapid restoration time resulting in a lower contact time of the drug with the absorptive membrane. As a result, the drug is washed away rapidly within 15–30 min after application and less than 5% of the dose reaches the target tissue.[3–5]

Conventional hypodermic treatments are used to overcome the challenges for the delivery of ophthalmic drugs to specific sites by either targeting the posterior or anterior segment of the eye. However, they are not preferred due to poor patient compliance, slow diffusion rate into the target tissue, pain and the need for well-skilled personnel to inject them into the eye. Moreover, multiple injections administration may cause more ocular complications for the patient.[6]

Implants have also been introduced for the treatment of glaucoma by reducing ocular pressure such as iStents,[7] Hydrus,[8] CyPass implant[9] and XEN Gel Stent.[10] Polymeric biodegradable or non-degradable implantable devices are considered as a very promising technology for sustained drug delivery directly to the cite of action. Moreover, lower drug concentrations are required to exert pharmacological action.[11, 12] However, implantable drug-loaded devices suffer from other challenges including the rapid initial release of drugs, increased drug concentration in the blood, ocular discomfort and patient non-compliance.[13]

Furthermore, timolol maleate has been used as a drug substance for delivery in contact lenses due to the clinical performance that has been demonstrated in clinical trials.[14–17] In most cases, contact lenses are fabricated using moulding process or molecular imprinting[15] where the drug is impregnated or soaked in the polymeric compositions.[18]

Three-dimensional (3D) printing is a versatile technology that has attracted significant attention from various industries including pharmaceutical,[19] biomedical,[20] food[21] and even construction.[22] Typical applications include transdermal drug delivery,[23, 24] prosthetics,[25, 26] microfluidics,[27] organs,[28, 29] and tumour models.[30, 31]

Some of the major features of 3D printing technologies include their capacity to fabricate structures with complex geometries with high accuracy, reproducibility and controlled drug release profiles rendering them suitable for personalised medications according to the patient clinical needs.[32–34]

The aim of this study was to design and fabricate drug-eluting contact lenses (DECL) using fusion deposition modelling (FDM) for the sustained delivery of timolol and the treatment of glaucoma. The technology was coupled with hot melt extrusion (HME)[35, 36] for the filament optimisation of ethylene-vinyl acetate copolymer (EVA) and polylactic acid (PLA) blends at various ratios in order to optimise printability and drug release rates. The study demonstrated promising results that could be used in the future treatment of glaucoma by printing personalised contact lenses.

Materials and Methods

Materials

PLA biopolymer granules were purchased from Goodfellow Cambridge Ltd (Huntingdon, England), EVA medical and non-medical grades were provided by Celanese (Germany). (S)-Timolol maleate (TML) was purchased from Hangzhou Longshine Bio-Tech Co., Ltd (Hangzhou, China).

Hot melt extrusion and 3D printing of drug-eluting contact lens

The EVA/PLA/TML physical blend at a ratio of 84 : 15 : 1 (wt/wt) was prepared and mixed using a turbula mixer (Glen Mills T2F Shaker/Mixer). The physical blend was fed into the hopper of a single screw hot melt extruder (Filabot EX6, Filabot HQ, USA). The extrusion temperatures across the screw barrel were set at 35°C, 160°C, 170°C and 140°C. The physical blend was extruded at 10 V using a 2.5 mm circular die. The extruded filament was passed through a cooling system consisting of five cooling fans and collected using a filament winder. The filament winding speed was adjusted to generate a filament with a desired diameter ranging from 2.6 to 2.9 mm suitable for FDM printing.

The contact lens was designed using SolidWorks 2015 (Dassault Systèmes). The lens dimensions were defined according to conventional marketed soft contact lenses (Air Optix Aqua) with 14.2 mm diameter. The thickness of the lens was adjusted at 0.26 mm with a 5 mm central aperture The contact lens design was converted into a stereolithography (stl) file and printed using a FDM 3D printer Ultimaker S5 (Ultimaker, the Netherlands). The contact lenses were printed using a 0.25 mm nozzle where the optimum printing settings were set to print temperature of 225°C, room temperature build plate, layer height of 40 µm, line width of 0.15 mm and print speed of 5 mm/s.

Differential scanning calorimetry (DSC)

The thermal behaviour of bulk materials and the drug-loaded filaments were studied using differential scanning calorimeter (Mettler Toledo 823e, Greifensee, Switzerland) and analysed using a DSC-1 Star System (Mettler Toledo Ltd, Greifensee, Switzerland). About 2–3 mg of each sample was carefully weighed and placed into a 40 µl aluminium pan and immediately crimped. The samples were examined using a heat-cool-heat cycle where heating and cooling rate were set at 10°C/min. The temperature range was adjusted from –40 to 240°C with a nitrogen flow rate at 50 ml/min.

Thermogravimetric analysis (TGA)

TGA (Q5000-IR, TA Instruments, Crawley, UK) was utilised to investigate the thermal stability of the bulk materials, plain and drug-loaded filaments. Approximately 2–3 mg of each sample was placed into a standard TGA aluminium pan. Each sample was heated in a nitrogen atmosphere at the heating rate of 10°C/min. The TGA curves were scanned from 25 to 500°C. Generated data were interpreted using TA Universal Analysis 2000 (TA Instruments, USA).

Rheology

The rheological behaviour of the pure polymers and extruded filaments across a wide range of shear rates was studied using an Anton Parr MCR 302 rheometer (Anton Parr GmbH, Graz, Austria). Rheological behaviour of all the samples was tested at a temperature of 200°C using an upper geometry of the 25-parallel plate. The samples were tested in a 1 mm gap from the upper geometry and the platform. The viscosity of the samples was examined from 0 s^{-1} to 100 s^{-1}. RheoCompass was used to analyse the extracted data.

Scanning electron microscopy (SEM)

The morphology of the 3D printing filaments was examined using Hitachi SU8030 cold-cathode field-emission gun SEM

(Hitachi High-Technologies, Germany). The samples were placed on an aluminium stub using double-sided black carbon tape. The images of the samples were taken at an accelerating voltage of IKV and ×30 magnification. The morphology of blank and drug-loaded contact lenses was investigated under low vacuum SEM. The samples were placed on an aluminium stub using double-sided black carbon tape. JEOL JSM 5310LV SEM (Tokyo, Japan) was used to examine the sample's morphology and 3D printed dimensions. Oxford Instruments Aztec software version 3.3 was used to montage the sample images.

X-ray diffraction (XRD)

Brucker D8 Advance diffractometer (Germany) equipped with a Göebel mirror using Cu-kα radiation was used to determine the crystallinity of TML within the extruded filament and the printed contact lens prototype using the transmission mode. The filament was carefully cut down into two small pieces using a sterile tweezer and placed into a metal holder covered with an X-ray transparent mylar sheet to hold the sample in place. The mylar coat was folded over the sample and placed into the transmission scanning stage. The diffractograms were collected between 5 and 60° 2θ with a scan speed at 0.2 s/step and a step size of 0.02° 2θ.

Mechanical testing

A texture analyser (TA, HD plus Texture Analyzer Stable Micro Systems Ltd, Surrey, UK) was used to investigate the mechanical properties of the extruded filaments. The TA was fitted with 30 kg load cell to assess the tensile strength of three distinct blend filaments. The total length of the sample was set to 120 mm and the gauge length was set to 80 mm. The specimens were put into custom-made 3D printed thermoplastic polyurethane grippers. The diameter of the filaments was recorded in five different locations of the specimen and the average diameter was used for calculations. The specimens were tested at a speed of 1 mm/s in accordance with ASTM D882 and D638 standard. The data were generated using the TA Exponent 32 software where each sample was evaluated in quintuplicate.

Drug release studies

Drug-loaded lenses containing 250 µg of TML were immersed in test tubes containing 15 ml of simulated tear fluid (STF, pH 7.4). The tubes were incubated in a water shaker bath under 120 rpm and kept at 37°C. During the study, 2 ml were withdrawn from each sample and replaced with equivalent fresh STF solution at predetermined intervals. Experiments were performed in triplicates. The TML concentration was determined using a Varian Cary 50 Bio-UV-visible spectrophotometer at room temperature. The concentration of the TML molecules released from the lenses was estimated using a calibration curve in STF at 295 cm^{-1}.[37]

Results and Discussion

Thermal characterisation

The DSC analysis of plain polymers, plain TML, EVA/PLA filaments and drug-loaded filaments, was conducted in order to identify the thermal events, the drug physical state and possible drug–polymer interactions.

As shown in Table 1, bulk PLA exhibited two endotherms where the first one is attributed to its glass transition at 57.93°C, while the secondary endothermic peak is related to the melting point at 149.78°C. The PLA also presented an exothermic peak at 98.00°C which is attributed to polymer crystallization. The non-medical EVA presented two endothermic events at temperatures of 50.41°C and 76.06°C which relates to the presence of two different types of crystals (polymorphs) in the EVA copolymer.[38]

EVA/PLA filament at 90 : 10 exhibited a shifted primary endotherm at 50.41°C suggesting polymer miscibility between EVA and PLA. In addition, the melting peak of PLA had a very weak endotherm response (small trace) which indicates strong interactions between the two polymers. In contrast, when the PLA ratio increased (EVA/PLA at 80 : 20 wt%) the melting endotherm of PLA appeared to be weak again indicating strong polymer–polymer interactions at such ratio.

As shown in Figure 1, the DSC thermogram of the plain medical EVA showed two endothermic events at around 45.90°C and 64.08°C, respectively, which comply with those of the non-medical grade EVA (Table 1). The thermogram of TML exhibited a single sharp endothermic event at 206.14°C, which relates to the melting endotherm. However, the melting endotherm disappeared in the TML-loaded filament suggesting that TML was converted into an amorphous state. Interestingly, the same thermogram showed a significant temperature depression of the two polymer endotherms at 39.09°C and 77.9°C which is greater compared with the shift observed for the polymer blends (Table 1). This can be possibly attributed to the formation of a glass solution where TML is molecularly dispersed in the polymer blends.

TGA studies were carried out to investigate the thermal stability of bulk materials and the filaments to evaluate the maximum temperature threshold for HME and 3D printing of the filaments. As shown in Figure 2, bulk PLA presented a single degradation temperature at 338°C, while both medical and non-medical EVA pellets presented a two-step degradation at 340°C due to loss of acetic acid and another degradation temperature at 450°C due to the loss of unsaturated polyethylene co-acetylene molecule.[39] Both EVA/PLA filaments presented a mass loss at 340–380°C due to the PLA decomposition and a second peak was observed between 400 and 500°C due to EVA's decomposition.

As shown in Figure 3, TML exhibited high thermal stability up to 201°C followed by a rapid mass loss due to the degradation.[40] Both drug-loaded filament and the drug-loaded 3D

Table 1 DSC analysis of bulk polymers and extruded filaments blends

Formulation (wt/wt)	Glass transition (°C)	Melting endotherms (°C)	Crystallization (°C)
PLA	57.93	150.88	98.00
Non-medical EVA	N/A	50.41 and 76.06	N/A
EVA/PLA filament 90 : 10	N/A	40.11 and 77.26	N/A
EVA/PLA filament 80 : 20	N/A	44.26 and 77.23	N/A

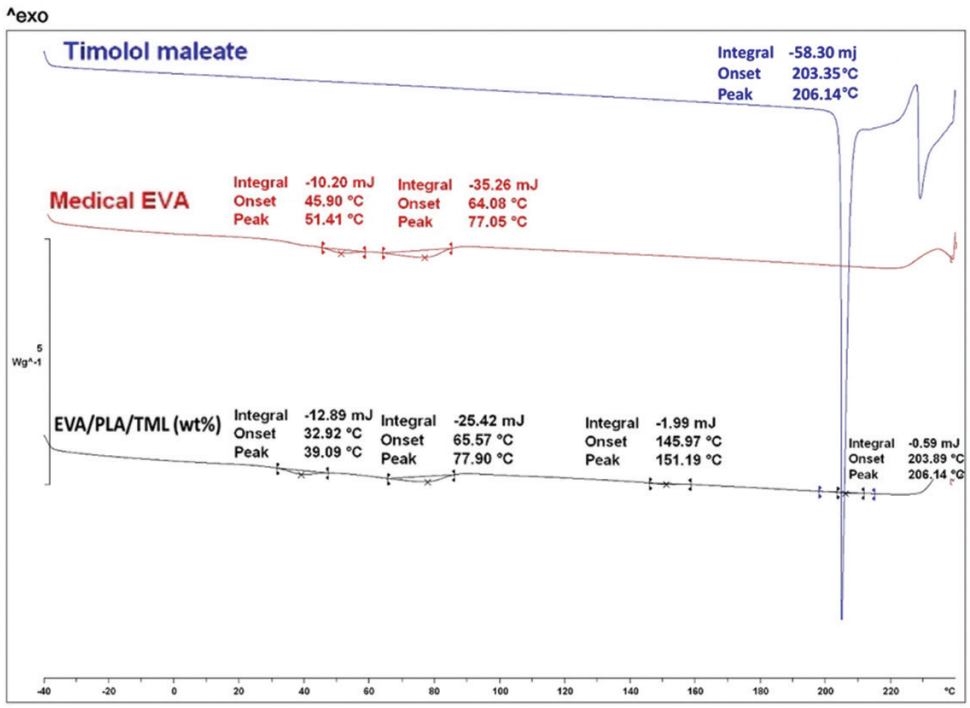

Figure 1 DSC thermograms of plain medical grade EVA, timolol maleate and timolol-loaded filament.

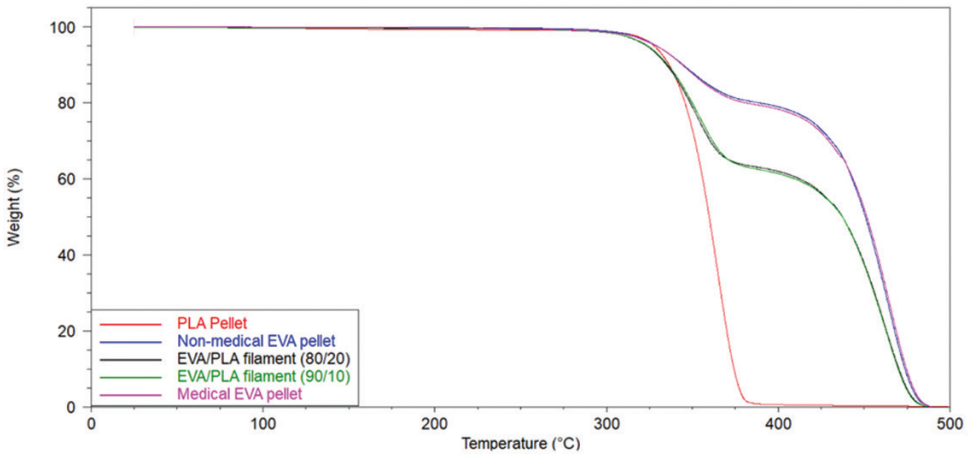

Figure 2 TGA of plain medical EVA, non-medical EVA, PLA and EVA/PLA filaments.

printed contact lens samples exhibited two-step mass loss which are mainly attributed to the raw polymeric materials of EVA and PLA and no apparent drug degradation is observed. The obtained TGA curves indicate that the drug has been protected from thermal degradation when embedded within the polymeric matrix through the HME process. Consequently, we were able to fabricate the drug-loaded contact lenses at relatively high temperature of 250°C while avoiding drug degradation.

X-ray analysis

As shown in Figure 4, X-ray analysis was conducted to investigate the solid state of the drug substance TML in the HME blend filament and the 3D printed contact lenses.

The XRD pattern shown in Figure 4 shows clear crystallinity of bulk TML with high-intensity peaks at 10°, 14°, 17°, 20°, 21° and 22°, 2θ. The XRD pattern of the TML-loaded filament showed that the drug was converted into an amorphous state. The presence of the amorphous drug in the extruded filaments is in good agreement with the DSC data described above.

Rheological studies

Rheological studies play an important role in processability settings of various 3D printing materials.[41] The study of the rheological behaviour of polymeric blends is highly required to determine the printability of the filaments. As shown in Figure 5, the viscosity of the 3D printing filaments was measured at printing temperatures, respectively, from shear rates of 0.1–100 s^{-1}.

All three formulations exhibited a shear thinning behaviour which is highly desirable for FDM applications.[36, 42] Both placebo filaments exhibited near-identical rheological behaviour. However, a slight increase in viscosity was observed by increase in the amount of the PLA. On the other hand, the drug-loaded filament exhibited increased viscosity at different

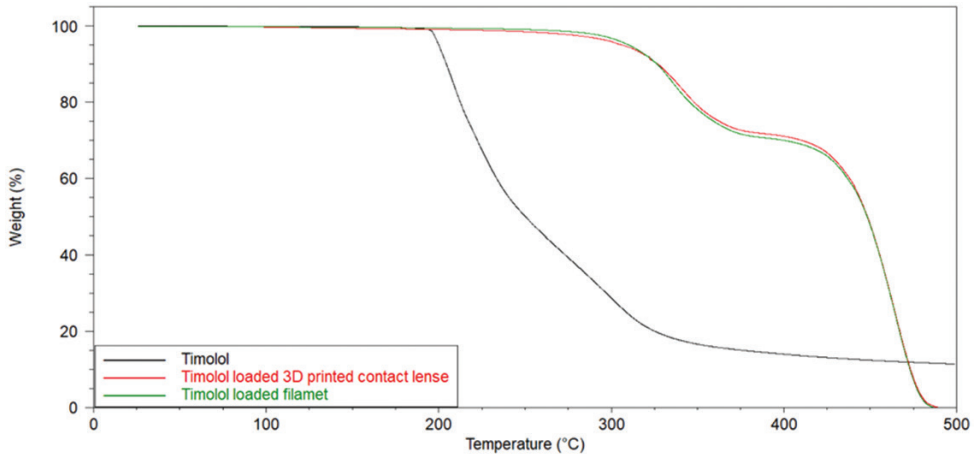

Figure 3 TGA of timolol-loaded filament and 3D printed timolol-loaded contact lens.

Table 2 Mechanical properties of the 3D printing filaments

Filament composition (wt/wt)	Ultimate tensile strength (MPa)	Percentage elongation (%)	Young's modulus (MPa)
EVA/PLA/TML (84/15/1)	58.94	398.22	101.96
EVA/PLA (90/10)	62.00	398.19	78.63
EVA/PLA (80/20)	112.78	517.62	114.96

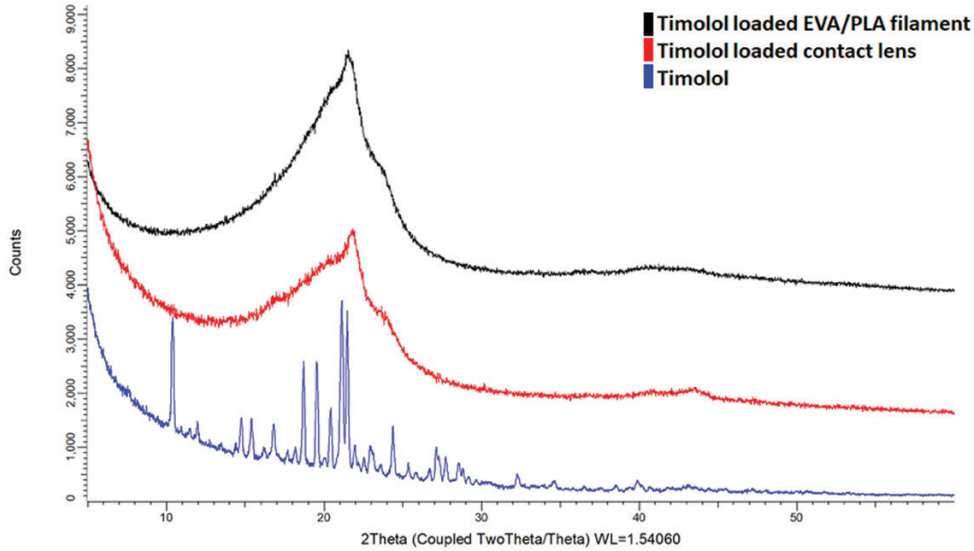

Figure 4 XRD graphs of timolol maleate, timolol-loaded 3D printing filament and timolol-loaded 3D printed contact lenses.

shear rates which is due to the presence of the EVA medical grade. Such high viscosity of the filament requires lower print speeds to ensure uninterrupted and continuous disposition of the filament through the nozzle as well as avoiding filament's crimping at the feeder section of the printer.

Mechanical studies

Tensile testing was carried out to investigate the printability of the fabricated 3D printing filaments (Table 2). According to a recent study,[36] filaments with ultimate tensile strengths of more than 17 MPa are considered printable. The tensile tests revealed that all three filament blends including the TML-loaded filament meet the ultimate tensile threshold of 17 MPa.

All three 3D printing filaments are quite flexible featuring high percentage elongation and low Young's modulus which is desirable for fabrication of contact lenses. As shown in Figure 6, the effect of TML in the extruded filaments was minimal and almost identical to the plain with EVA/PLA 90 : 10 (wt/wt). There is a slight increase in rigidity (Young's modulus) of the timolol-loaded filament in comparison with the placebo filament (EVA/PLA 90 : 10) which is explained due to differences in mechanical behaviour of medical and non-medical EVA grades. Nevertheless, consideration for the printability of the filaments should be taken into account due to possible feeding of over flexible filaments according to Nasereddin *et al.*[43] Therefore, low print speeds were used for printing of the contact lenses to avoid crumbling the filaments.

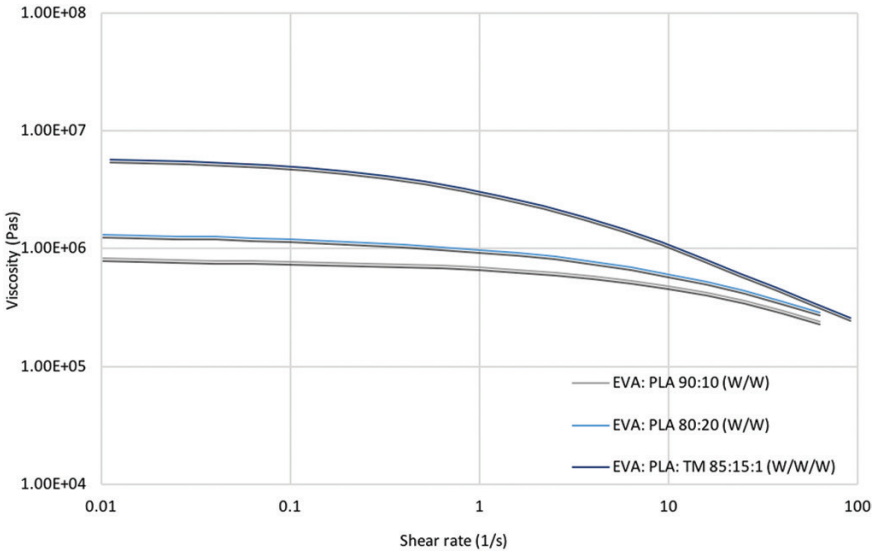

Figure 5 Viscosity measurements EVA/PLA filaments and timolol-loaded filaments.

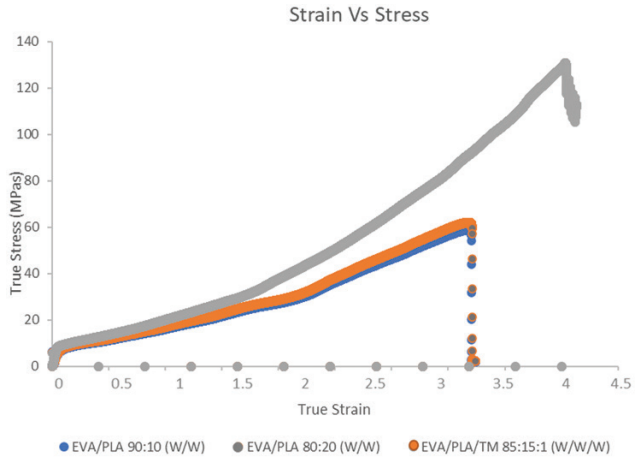

Figure 6 Stress–strain graphs of EVA/PLA and timolol-loaded filaments.

Hot melt extrusion and 3D printed contact lenses

The mechanical pushing mechanism used in the FDM printers to propel the filament towards the heating zone requires thermoplastic materials with a specific limit of mechanical strength that guarantees the proper material feeding without any difficulty which might lead to nozzle blockage and eventually cause printing process failure. For instance, materials with inadequate mechanical strength exhibit bending behaviour resulting in grinding the filament in between the moving rotating rollers during the feeding process. On the other hand, very ductile materials may exhibit fractures at the feeding zone that also leads to the failure of the process.

The pure EVA filaments (data not shown) lacked sufficient mechanical strength despite the fact that they fulfil all the other required features. Therefore, we found that it was challenging to achieve the desired printability from bulk EVA. As a result, another trial was conducted to extrude EVA/PLA blends to improve the mechanical characteristics of EVA polymers. The EVA/PLA were blended at ratios of 90 : 10 (w/w) which improved the mechanical strength without compromising the transparency of EVA. The extruded EVA/PLA of ratio at 90 : 10 (wt/wt) was fed successfully into the feeder and extruded from the nozzle's tip. Although successfully printing contact lenses, the particular blend presented the same issues of grinding, under extrusion and nozzle blockage during printing.

As a result, a new EVA/PLA 80 : 20 (wt/wt) blend was extruded using the same extrusion setting parameters. In comparison with EVA/PLA blend of 90 : 10 (w/w), it was observed that the feeding of filament into the printer was much easier and the printing reproducibility was improved while grinding, buckling and irregular extrusion problems rarely occurred. Even though the successful printing attempts of the contact lens was achieved using EVA/PLA 80 : 20 (wt/wt), the contact lenses exhibited lower flexibility and showed crack marks upon bending in comparison with contact lenses printed using EVA/PLA at 90 : 10 (w/w) ratio. Therefore, the 80 : 20 (w/w) ratio of EVA/PLA was selected for the drug loading step but using medical grade EVA polymer. For the drug-loaded filament, further experimentation (data not shown) revealed that extruded blends of EVA/PLA/TML at 84/15/1 (w/twt/wt) ratio could be used for 3D printing processing. The new blend composition was fed smoothly into the printer's feeder and printing attempts were successful.

The initial printing trials revealed the printing of contact lenses was very challenging without using support material due to the inherent overhang of the contact lens model. Polyvinyl alcohol (PVA) was used as a support material and fed into the second extruder to support the lens internally. PVA was particularly chosen as a suitable material due to its ease of removal from the printed lenses because of its high-water solubility. As a result, the support was easily removed off by simply immersing the lens in a beaker filled with water and left for around 2 h until the PVA material attached to the lens was completely dissolved. PVA exhibited a good fusion with the main printing blend of EVA/PLA material. However, the print quality was not optimal on the upper part of the lens. Although printing with support has assisted to overcome the overhang issue in the lens model, it compromised the lens transparency and printing time was prolonged.

As Figure 7 illustrates, two lens structures with or without an aperture were designed using SolidWorks 2015 CAD software at dimensions of 12 mm in diameter and thickness of

Figure 7 Blank 3D printed contact lenses with and without central aperture (5 mm) comprising of EVA/PLA 90 : 10 (wt/wt) blend.

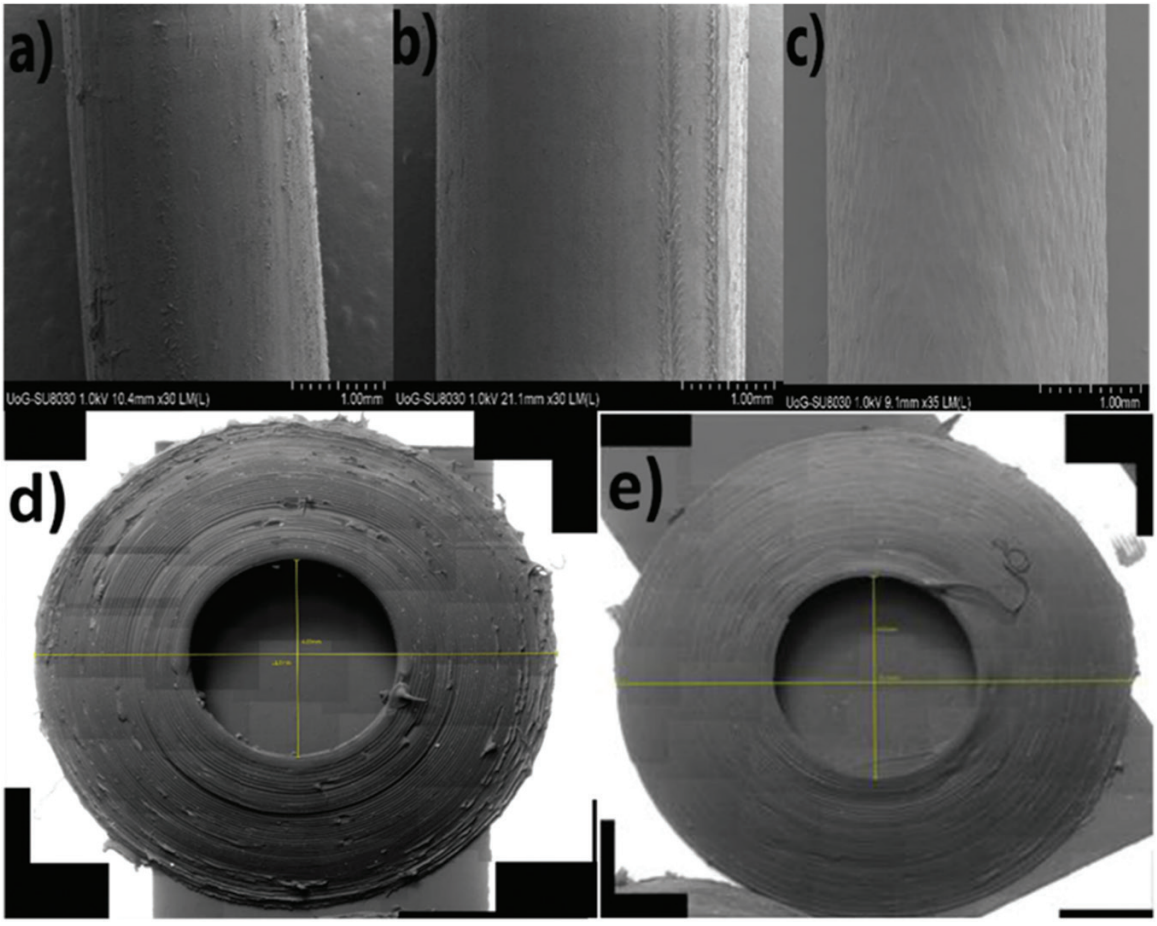

Figure 8 SEM images of (a) EVA/PLA 90 : 10 (wt/wt), (b) EVA/PLA 80 : 20 (wt/wt), and (c) timolol-loaded EVA/PLA 3D printing filament at 84 : 15 : 1 (wt/wt). SEM images of (d) 3D printed timolol-loaded and (e) placebo contact lenses.

0.26 mm and saved as STL format. During the print optimisation, it was decided that the lens design with circular 5 mm aperture was decided as the best option for DECL in order to avoid the improper vision of the patient when applied on the eye. The drug-loaded filament of EVA/PLA/TML at 8 : 15 : 1 (wt/wt/wt) ratio was successfully used for printing lenses which showed a yellowish colour due to the melting of the drug during printing. Further investigation showed that printing below the melting point of the drug at 200°C the lenses appeared transparent, without forming the yellowish colour.

As shown in Supplementary Table 1, for the printing optimisation of 3D printed contact lenses, the most important print setting parameters were investigated including nozzle diameter, thickness layer, line width, print speed, printhead size and build-plate temperatures. Due to the hollow structure of lens design, the infill ratio has no major effect on the printing

quality. However, infill is one of the FDM setting parameters which can affect the rate of drug release. It has been reported that faster release rates of drugs have been observed in some printed drug-loaded dosage forms with higher infill percentages.[44] In addition, print speed and layer thickness influence the quality of 3D structures.

Furthermore, our printing optimisation showed that lower print speed and layer thickness results in the fabrication of 3D structures with higher resolution and better quality.[19] In this respect, a smaller nozzle's diameter of 0.25 mm was used for lens printing instead of a 0.4 mm nozzle in order to obtain very fine layers of deposited materials and achieve a very smooth surface with invisible lines. Additionally, the nozzle temperature is a very important factor in FDM printing technology as the filament should be heated at temperatures above its glass transition or melting point of the polymer to adequately melt the material and easily extrude it from the nozzle. The use of higher printing temperatures above the melting point of material is usually recommended to overcome the slight shear force applied to the molten material during extrusion from the nozzle. In this sense, the difference of temperatures applied in HME and 3D printing could reach 100°C depending on different materials.[45] This is because the shear thinning behaviour improves the flow efficiency of the filament and the energy consumed during processing.[46] Successful printings have been achieved at temperatures of 220–225°C using the EVA/PLA blends containing non-medical grade of EVA. In contrast, the EVA/PLA blend filament containing medical grade of EVA exhibited successful printing behaviour at temperatures starting from 200°C.

Scanning electron microscopy (SEM) analysis

The SEM images of HME extruded filaments of EVA/PLA blends at 90 : 10 and 80 : 20 (wt/wt) along with TML-loaded filament shown in Figure 8a–c exhibited smooth and consistent surface morphology with no defects.

As shown in Figure 8e, the morphology of the blank 3D printed contact lens using EVA/PLA blend (90 : 10, wt/wt) presented better consistency and smoother surface in comparison with TML-loaded printed contact lens. However, the differences in print layer consistency between the samples could be attributed to the use of different EVA grades where in this study the placebo contact lenses were printed using non-medical EVA grades while the drug-loaded using a medical grade EVA. As shown in Figure 8e and d, the surfaces of the placebo and drug-loaded 3D printed contact lenses feature some zits and blobs due to the frequent movement and stops of the print head around the print. Hence, future optimisation is needed in order to improve the surface characteristics of the printed drug-loaded lenses.

As shown in Table 3, the theoretical values for the lens aperture and external diameter should be around 5 and 12 mm, respectively, according to the CAD designs. However, the recorded measurements from the SEM images showed slightly smaller values due to the inherent tendency of thermoplastic materials to shrink in the cooling step during the printing process.

Furthermore, Figure 9 shows the top view of the drug-loaded lens that present adequate consistency among the printed layers and excellent intralayer adhesion.

Drug release studies

An objective of the study was to optimise drug-eluting lenses that would provide sustained release rates of TML for a period of 7 days. As shown in Figure 10, most of TML was released after 24 h and a burst release of 20% was observed within the first 5 h.

Table 3 External and aperture's diameter measurements in millimetres for placebo and drug-loaded contact lenses

Design	Internal diameter (mm)	External diameter (mm)	CAD internal diameter (mm)	CAD external diameter (mm)	Internal diameter tolerance (%)	External diameter tolerance (%)
Placebo lens	4.69	11.8	5.0	12.0	6.2	1.6
Timolol leaded lens	4.65	11.5	5.0	12.0	7.0	4.1

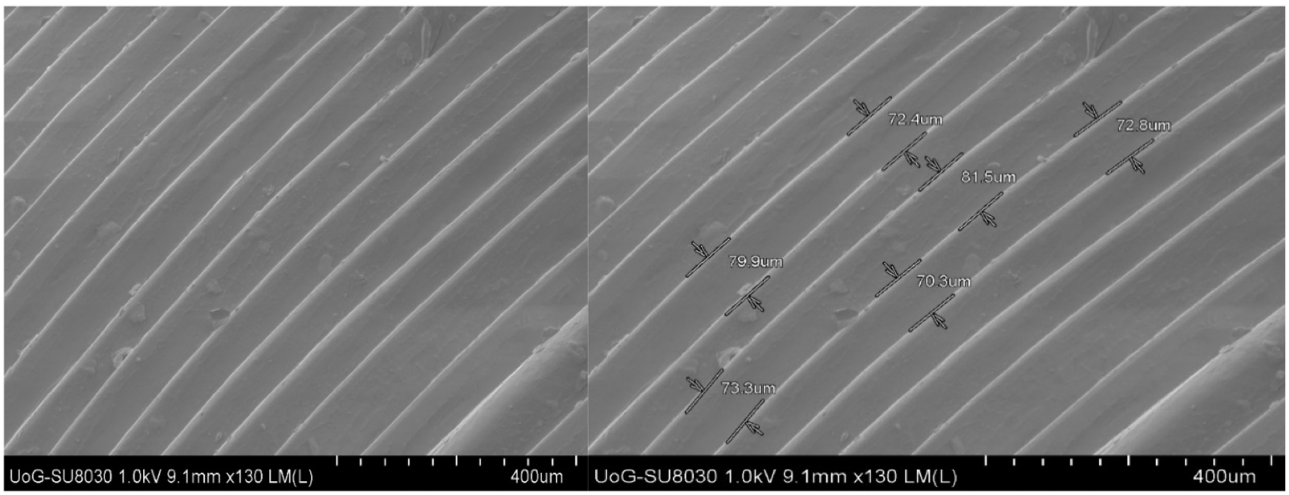

Figure 9 SEM images of cross-sections of drug-loaded contact lens with and without layer thickness measurements.

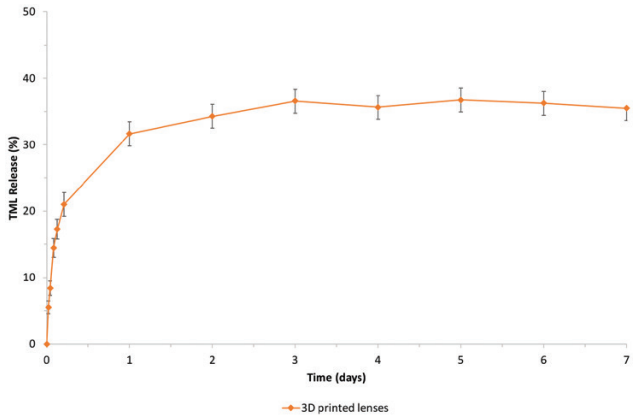

Figure 10 TML release from 3D printed contact lenses.

The burst release was attributed to the localised TML on the surface of the lenses. In addition, the drug release occurred only for 3 days where 35% was detected followed by negligible release for the remaining period of the study. From the release pattern, it is obvious TML sustained release was not achieved mainly due to the slow diffusion from the polymer matrix. Hence, further work is required to optimise the drug release at the desired rate (around 50 µg/day). This can be either achieved through the addition of hydrophilic polymer (plasticisers) in the EVA/PLA blends or by using different EVA/PLA grades of low molecular weights.

Conclusions

In this study, 3D printing technology was coupled with HME processing for the development of EVA/PLA/TML printable blends and the printing of drug-eluting blends. The extruded filaments presented suitable printability while the drug-loaded lenses showed a smooth surface. The TML release rates were limited for only 3 days while a burst release was observed. Nevertheless, the study demonstrated that the design and printing of drug-eluting lenses is feasible but further work is required for drug release optimisation.

Supplementary Material

Supplementary data are available at *Journal of Pharmacy and Pharmacology* online.

Author Contributions

Conceptualisation: J.S.B. and D.D. Methodology: Y.M.G.M., A.G.T., M.T., U.N., R.K. and I.A. Formal analysis: Y.M.G.M., A.G.T., M.T., U.N. and D.D. Investigation: Y.M.G.M., A.G.T., M.T., U.N., R.K. and I.A. Data curation: Y.M.G.M., A.G.T. and D.D. Writing – original draft preparation: Y.M.G.M., A.G.T. and D.D. Review and editing: A.G., J.S.B. and D.D. Project administration: D.D.

Funding

This research received no specific grant from any funding agency in the public, commercial, or not-for-profit sectors..

Conflict of Interest

None declared.

References

1. Conlon R, Saheb H, Ahmed IIK. Glaucoma treatment trends: a review. *Can J Ophthalmol* 2017; 52: 114–24. https://doi.org/10.1016/j.jcjo.2016.07.013
2. Weinreb RN, Aung T, Medeiros FA. The pathophysiology and treatment of glaucoma: a review. *JAMA* 2014; 311: 1901–11. https://doi.org/10.1001/jama.2014.3192
3. Ahmed I. The noncorneal route in ocular drug delivery. In Mitra AK (ed.), *Ophthalmic Drug Delivery Systems*. 2nd edn. Boca Raton, FL: CRC Press, 2003, 356–85.
4. Gaudana R, Ananthula HK, Parenky A *et al*. Ocular drug delivery. *AAPS J* 2010; 12: 348–60. https://doi.org/10.1208/s12248-010-9183-3
5. Gipson IK, Argüeso P. Role of mucins in the function of the corneal and conjunctival epithelia. *Int Rev Cytol* 2003; 231: 1–49. https://doi.org/10.1016/s0074-7696(03)31001-0
6. Thakur Singh RR, Tekko I, McAvoy K *et al*. Minimally invasive microneedles for ocular drug delivery. *Expert Opin Drug Deliv* 2016; 14: 525–37. https://doi.org/10.1080/17425247.2016.1218460
7. Belovay GW, Naqi A, Chan BJ *et al*. Using multiple trabecular micro-bypass stents in cataract patients to treat open-angle glaucoma. *J Cataract Refract Surg* 2012; 38: 1911–7. https://doi.org/10.1016/j.jcrs.2012.07.017
8. Camras LJ, Yuan F, Fan S *et al*. A novel Schlemm's Canal scaffold increases outflow facility in a human anterior segment perfusion model. *Invest Ophthalmol Vis Sci* 2012; 53: 6115–21. https://doi.org/10.1167/iovs.12-9570
9. Hoeh H, Vold SD, Ahmed IK *et al*. Initial clinical experience with the CyPass micro-stent. *J Glaucoma*. 2016; 25: 106–12. https://doi.org/10.1097/ijg.0000000000000134
10. Grover DS, Flynn WJ, Bashford KP *et al*. Performance and safety of a new ab interno gelatin stent in refractory glaucoma at 12 months. *Am J Ophthalmol* 2017; 183: 25–36. https://doi.org/10.1016/j.ajo.2017.07.023
11. Dash AK, Cudworth GC. Therapeutic applications of implantable drug delivery systems. *J Pharmacol Toxicol Methods* 1998; 40: 1–12. https://doi.org/10.1016/S1056-8719(98)00027-6
12. Rajgor N, Patel M, Bhaskar VH. Implantable drug delivery systems: an overview. *Syst Rev Pharm* 2011; 2: 91–5. https://doi.org/10.4103/0975-8453.86297
13. Manickavasagam D, Oyewumi MO. Critical assessment of implantable drug delivery devices in glaucoma management. *J Drug Deliv* 2013; 2013: 895013. https://doi.org/10.1155/2013/895013
14. Desai AR, Maulvi FA, Pandya MM *et al*. Co-delivery of timolol and hyaluronic acid from semi-circular ring-implanted contact lenses for the treatment of glaucoma: in vitro and in vivo evaluation. *Biomater Sci* 2018; 6: 1580–91. https://doi.org/10.1039/c8bm00212f
15. Hiratani H, Fujiwara A, Tamiya Y *et al*. Ocular release of timolol from molecularly imprinted soft contact lenses. *Biomaterials* 2005; 26: 1293–8. https://doi.org/10.1016/j.biomaterials.2004.04.030
16. Hsu KH, Carbia BE, Plummer C *et al*. Dual drug delivery from vitamin E loaded contact lenses for glaucoma therapy. *Eur J Pharm Biopharm* 2015; 94: 312–21. https://doi.org/10.1016/j.ejpb.2015.06.001
17. Maulvi FA, Patil RJ, Desai AR *et al*. Effect of gold nanoparticles on timolol uptake and its release kinetics from contact lenses: *in vitro* and *in vivo* evaluation. *Acta Biomater* 2019; 86: 350–62. https://doi.org/10.1016/j.actbio.2019.01.004
18. Tian C, Zeng L, Tang L *et al*. Sustained delivery of timolol using nanostructured lipid carriers-laden soft contact lenses. *AAPS PharmSciTech* 2021; 22: 212. https://doi.org/10.1208/s12249-021-02096-6

19. Norman J, Madurawe RD, Moore CM *et al*. A new chapter in pharmaceutical manufacturing: 3D-printed drug products. *Adv Drug Deliv Rev* 2017; 108: 39–50. https://doi.org/10.1016/j.addr.2016.03.001
20. Ahangar P, Cooke ME, Weber MH *et al*. Current biomedical applications of 3D printing and additive manufacturing. *Appl Sci* 2019; 9: 1713. https://doi.org/10.3390/app9081713
21. Kumar P, Kumar P, Kumar R. 3D printing of food materials: a state of art review and future applications. *Mater Today Proc* 2020; 33: 1463–7. https://doi.org/10.1016/j.matpr.2020.02.005
22. Albar A, Chougan M, Al-Kheetan MJ *et al*. Effective extrusion-based 3D printing system design for cementitious-based materials. *Results Eng* 2020; 6: 100135. https://doi.org/10.1016/j.rineng.2020.100135
23. Economidou SN, Pere CPP, Reid A *et al*. 3D printed microneedle patches using stereolithography (SLA) for intradermal insulin delivery. *Mater Sci Eng C Mater Biol Appl* 2019; 102: 743–55. https://doi.org/10.1016/j.msec.2019.04.063
24. Pere CPP, Economidou SN, Lall G *et al*. 3D printed microneedles for insulin skin delivery. *Int J Pharm* 2018; 544: 425–32. https://doi.org/10.1016/j.ijpharm.2018.03.031
25. Koprnický J, Najman P, Šafka J. 3D printed bionic prosthetic hands. In *2017 IEEE International Workshop of Electronics, Control, Measurement, Signals and Their Application to Mechatronics (ECMSM)*, 24–26 May 2017, Donostia, Spain, 2017, 1–6.
26. Vujaklija I, Farina D. 3D printed upper limb prosthetics. *Expert Rev Med Devices* 2018; 15: 505–12. https://doi.org/10.1080/17434440.2018.1494568
27. Waheed S, Cabot JM, Macdonald NP *et al*. 3D printed microfluidic devices: enablers and barriers. *Lab Chip* 2016; 16: 1993–2013. https://doi.org/10.1039/c6lc00284f
28. Faulkner-Jones A, Fyfe C, Cornelissen DJ *et al*. Bioprinting of human pluripotent stem cells and their directed differentiation into hepatocyte-like cells for the generation of mini-livers in 3D. *Biofabrication* 2015; 7: 044102. https://doi.org/10.1088/1758-5090/7/4/044102
29. Tabriz AG, Hermida MA, Leslie NR *et al*. Three-dimensional bioprinting of complex cell laden alginate hydrogel structures. *Biofabrication* 2015; 7: 045012. https://doi.org/10.1088/1758-5090/7/4/045012
30. Datta P, Dey M, Ataie Z *et al*. 3D bioprinting for reconstituting the cancer microenvironment. *NPJ Precis Oncol* 2020; 4: 18. https://doi.org/10.1038/s41698-020-0121-2
31. Zhao Y, Yao R, Ouyang L *et al*. Three-dimensional printing of Hela cells for cervical tumor model *in vitro*. *Biofabrication* 2014; 6: 035001. https://doi.org/10.1088/1758-5082/6/3/035001
32. Castellano JM, Sanz G, Peñalvo JL *et al*. A polypill strategy to improve adherence: results from the FOCUS project. *J Am Coll Cardiol* 2014; 64: 2071–82. https://doi.org/10.1016/j.jacc.2014.08.021
33. Scoutaris N, Ross SA, Douroumis D. 3D printed "Starmix" drug loaded dosage forms for paediatric applications. *Pharm Res* 2018; 35: 34. https://doi.org/10.1007/s11095-017-2284-2
34. van Lith R, Baker E, Ware H *et al*. 3D-printing strong high-resolution antioxidant bioresorbable vascular stents. *Adv Mater Technol* 2016; 1: 1600138. https://doi.org/10.1002/admt.201600138
35. Ghanizadeh Tabriz A, Nandi U, Hurt AP *et al*. 3D printed bilayer tablet with dual controlled drug release for tuberculosis treatment. *Int J Pharm* 2020; 593: 120147. https://doi.org/10.1016/j.ijpharm.2020.120147
36. Tabriz AG, Scoutaris N, Gong Y *et al*. Investigation on hot melt extrusion and prediction on 3D printability of pharmaceutical grade polymers. *Int J Pharm* 2021; 604: 120755. https://doi.org/10.1016/j.ijpharm.2021.120755
37. Ramachandran S, Tseng Y, Yu YB. Repeated rapid shear-responsiveness of peptide hydrogels with tunable shear modulus. *Biomacromolecules* 2005; 6: 1316–21. https://doi.org/10.1021/bm049284w
38. Almeida A, Possemiers S, Boone MN *et al*. Ethylene vinyl acetate as matrix for oral sustained release dosage forms produced via hot-melt extrusion. *Eur J Pharm Biopharm* 2011; 77: 297–305. https://doi.org/10.1016/j.ejpb.2010.12.004
39. Costache MC, Jiang DD, Wilkie CA. Thermal degradation of ethylene-vinyl acetate coplymer nanocomposites. *Polymer* 2005; 46: 6947–58. https://doi.org/10.1016/j.polymer.2005.05.084
40. Mehta P, Al-Kinani AA, Haj-Ahmad R *et al*. Electrically atomised formulations of timolol maleate for direct and on-demand ocular lens coatings. *Eur J Pharm Biopharm* 2017; 119: 170–84. https://doi.org/10.1016/j.ejpb.2017.06.016
41. Cicala G, Giordano D, Tosto C *et al*. Polylactide (PLA) filaments a biobased solution for additive manufacturing: correlating rheology and thermomechanical properties with printing quality. *Materials (Basel)* 2018; 11: 1191. https://doi.org/10.3390/ma11071191
42. Elbadawi M, Gustaffson T, Gaisford S *et al*. 3D printing tablets: predicting printability and drug dissolution from rheological data. *Int J Pharm* 2020; 590: 119868. https://doi.org/10.1016/j.ijpharm.2020.119868
43. Nasereddin JM, Wellner N, Alhijjaj M *et al*. Development of a simple mechanical screening method for predicting the feedability of a pharmaceutical FDM 3D printing filament. *Pharm Res* 2018; 35: 151. https://doi.org/10.1007/s11095-018-2432-3
44. Goyanes A, Det-Amornrat U, Wang J *et al*. 3D scanning and 3D printing as innovative technologies for fabricating personalized topical drug delivery systems. *J Control Release* 2016; 234: 41–8. https://doi.org/10.1016/j.jconrel.2016.05.034
45. Melocchi A, Parietti F, Maroni A *et al*. Hot-melt extruded filaments based on pharmaceutical grade polymers for 3D printing by fused deposition modeling. *Int J Pharm* 2016; 509: 255–63. https://doi.org/10.1016/j.ijpharm.2016.05.036
46. Jaggi HS, Satapathy BK, Ray AR. Viscoelastic properties correlations to morphological and mechanical response of HDPE/UHMWPE blends. *J Polym Res* 2014; 21: 482. https://doi.org/10.1007/s10965-014-0482-8.